Journal of Petroleum Science and Technology 10 (4), 2020, Pages 31-40
DOI:10.22078/jpst.2020.4150.1671

Journal of Petroleum Science and Technology

https://jpst.ripi.ir/

Improving the Petrophysical Evaluation and Fractures Study of Dehram Group Formations Using Conventional Petrophysical Logs and FMI Image Log in one of the Wells of South Pars Field

Kioumars Taheri[1]* and Ali Hadadi[2]

[1]*Petroleum Exploration Engineering, Department of Mining and Metallurgicl Engineering, Yazd University, Yazd, Iran*

[2]*Petroleum Exploration Engineering, Dempartment of Petroleum Engineering, Islamic Azad University, Centeral Tehran Branch, Iran*

Abstract

The South Pars gas field is one of the southwestern fields of Iran. This field in the Zagros sedimentary basin and consists of two Kangan and Dalan reservoirs. The Kangan and Dalan Formations belong to Dehram Group, and they are the most significant gas reservoirs in the Persian Gulf area. In this research, exploratory and production well data in the South Pars gas field were examined. Moreover, Fracture and reservoir parameters were investigated through from petrophysical logs, FMI image log, and the litholog. Additionally, according to the lithology, shale volume, presence of evaporite sediments, and porosity, the Kangan Formation to K1 and K2, and the Dalan Formation have been zoned to K3 and K4 sections. Furthermore, fractures are essential for the initial migration of hydrocarbons from the source rock to the reservoir, and this study tries to provide useful information for the future. According to FMI log analysis, about 200 Fractures have been detected in Kangan and Upper Dalan reservoir intervals in the studied well up to now. Of which, 2 breakouts, 2 tensile fractures, 4 closed fractures, 19 open fractures, 63 beddings, 2 cross beddings, 35 conductive fractures, 26 stylolites, 47 unclassified fractures have been visible in the results. The findings of this study showed that zones K2 and K4 with the highest porosity and the lowest amount of water saturation have a higher reservoir quality than zones K1 and K3 sections. Also, the K4 zone has had the highest fracture density in comparison to other zones, which leads to increased porosity of the zone. Ultimately, zone K2 with the least thickness (43 meters) had a lower fracture density in comparison with the K4 zone (7 conductive fissures and 2 open fractures). Also, in comparison with other zones, it has low water saturation and high porosity and has a higher reservoir quality than K3 and K1 zones.

Keywords: Kangan Formation, Dalan Formation, South Pars field, Petrophysical evaluation, FMI image log.

Introduction

The Persian Gulf is considered a shallow basin in comparison with other marine basins in the world with similar potential, which it menas that lower drilling and other services are cost-effective. Additionally, Kangan and Dalan formations are in Dehram group with the age of Late Permian and Early Triassic, and they are known as the most significant gas reservoirs in either the Persian Gulf or the world [1]. Moreover, the number of gas reserves in the Iranian section of the field is 14 trillion cubic meters, which it makes up 8 percent of the gas of the world and 40 percent of gas reserves of Iran. Therefore, any investigation in this area will lead to a better understanding of this basin, and help to reduce the operational costs.

Several studies have been carried out by some researchers in the petrophysical assessments and fracture field. These studies, some of which have been referred to, include geological, hydrocarbon, and geophysical data. The stratigraphy of the Dalan and Kangan Formations in the Dehram Group was studied by Szabo and kheradpir. By investigating the outcrops (Mount Surmeh and Mount Faragoon) and terrestrial sections (Kooh Siah), the Dalan and the Kangan formations were introduced, and it was concluded that at the Zagros Highlands due to pre-Jurassic erosion, the Kangan Formation is not usually observed [2]. The identification of 3D modeling of fluid loss regions using the improved Gustafson-Kessel fuzzy clustering algorithm was conducted by Taheri and Morshedy. Therein, three-dimensional fuzzy zoning was executed, and the Fisher's model discriminant analysis

**Corresponding author:* Kioumars Taheri, National Iranian South Oilfields Company, Department of Geology, (NISOC), Ahvaz, Iran

E-mail addresses: kio.taheri@yahoo.com, kio.taheri@stu.yazd.ac.ir

Received 2020-04-21, Received in revised form 2020-09-29 , Accepted 2020-10-26, Available online 2021-03-16

proved that the obtained zoning from the clustering method has a better performance than the common geological zoning for modeling and zoning the mud loss [3]. Later, the South Pars gas field from the perspective of organic geochemistry and its gas reservoir origin was studied by Aali and the colleagues. It has been found out that the origin of the Dehram gas reservoirs in the South Pars field is gas migration from the Silurian source rock (Sarchahan Formation) [4]. Furthermore, the impact of events on the Permutrias boundary on the quality of the Dalan and Kangan Formation reservoirs in South Pars field was investigated by Rahimpour and colleagues, and it was concluded that the sedimentary sequence comprises limestone, dolomite, and evaporates that have been homologated in the interior to the middle parts of a carbonate ramp [5]. Soleimani and colleagues performed integrated petrophysical modeling for a completely heterogeneous and broken reservoir. In their study, zone 2 of Sarvak Formation was decided as a production zone with better performance of reservoir rock as a consequence of its maximum porosity [6]. Also, the congestion of fractures of the fractured area using sonic petrophysical logs and fracture density was determined by Tokhmchi et al. Therein, nonlinear regression was found with application of a generalized estimator that computes the fracture density with a correlation coefficient higher than 80% [7]. Furthermore, simulation was used by Soleimani to study a broken reservoir. In this study, which used the elastic fracture model, the results showed an elastic gridded model could better simulate reservoir performance [8]. The density of fractures using the petrophysical logs and a neuro-fuzzy system has been obtained by Jafari et al, which it has led to high compatibility (a correlation coefficient of 98%) between the estimated fracture density and the neuro-fuzzy value [9]. The permeability and fracture densities utilizing petrophysical logs have been estimated by Abdideh et al, and simultaneously, the depth of the fractures was determined. The results indicated that the accumulation of fractures decreases in the lower zones of the reservoir [10]. Moreover, a study with the aim of well performance optimization for gas lift operation in a heterogeneous reservoir by application of fine zonation was conducted by Soleimani. Accordingly, the findings cliam that a 7% change in production index will make 4% changes in optimal gas flow rate value [11].

Shahinpour has interpreted the sedimentary environments and the shale volume by analyzing the Fullbore Micro-Imager (FMI) in an exploratory well in the North Sea, which it has led to the identification of sedimentary layering, lithology, sedimentary environment, and the calculation of the shale volume [12]. Following these studies, the Permo-Triassic obstacles inside the reservoir of the South Pars field by the mean of petrophysical logs were evaluated by Rahim Pourbonab et al. The identification of three obstacles inside the reservoirs, including diagenesis sedimentations and sequence stratigraphy were among their significant findings [13]. The facies, sedimentary environment, and sequence stratigraphy of Dalan formation in the South Pars field have been investigated by Naser Rezavand et al. In addition, some results such as the identification of 15 microfacies in 5 separate environments of tidal, lagoon, barrier, Open Marine, and middle sectors of the homoclinic carbonate ramp have been achieved by them.

Also, the most important diagenetic processes which are dissolution, calcite cement, dolomitization, anhydritization, and physical and chemical density have been identified by them [14]. Then, the fractures of the Asmari Reservoir using the modeling performed on the drilling mud loss and the FMI image log have been studied by Taheri et al. The type of reservoir fracture distributionby investigating the effects of these fractures on the porosity and permeability of the reservoir rock has been specified by them [15]. Moreover, 3D qualitative fractures using the tomography of the industrial calculations have been analyzed by Lai et al. The results have illustrated that the utilization of ICT has the advantage of 3D imaging of the fractures without destruction [16]. a research to identify the fractures of the Asmari Formation using the FMI log and petrophysical data has been perforemed by Aghli et al. It indicates that the FMI and EMI logs are suitable for the evaluation of the reservoir, and the fracture parameters in the coreless wells [17].

For this project, geological maps, field reports, and raw data on the subject of research have been collected. Also, cores, drill bits, and Kagan and Dalan units through field excavations and estimates of lithological units were evaluated and studied in the well. Further, Petrophysics logs such as gamma (GR), acoustic (DT), density (RHOB), and neutron (NPHI) were loaded. Additionally, Petrophysical logs were defined to determine lithology, calculate shale volume, porosity, and water saturation. Then, with FMI logging the fractures were analyzed, after which detailed results were obtained, and finally zoning and determination of the reservoir quality of the studied field was performed. The purpose of this study is to analyze the structural and fracture density and their impact on the reservoir quality. In the Kangan and Dalan Formations to determine petrophysical parameters from image log data used. This data such as fluids saturation calculation, porosity, shale volume, and lithology in the examined studying wells of South Pars field using petrophysical logs.

Geological Setting

South Pars Gas Field is just a part of the largest gas field in the world.Geographically, it is positioned in the eastern longitude of 52–52.5° and 26.5–27° north latitude. This field is located in 100 km south of Assaluyeh port (75 km from Kish), and on the Iran-Qatar joint border line, with an area of about 9700 square kilometers. The area of this field is 3700 km in the Iranian section and 6000 km in Qatar country. The length and width of the field is approximately 150 km and 70 km respectively, while the northern part of the field is known as the North Dome, and it is located in the waters of Qatar. The amount of gas which has been reserved in the Iranian section of the field is 464 trillion cubic feet, which makes up 8 percent of the world's gas and 40 percent of Iran's gas reserves. In this field, the average recovery per well is estimated at 2 million cubic feet per day. The gas basin in this field in the Persian Gulf is divided into two parts of the northwest and southeast, as seen in Figure 1.

The cut pattern of Kangan limestone formation in well number 1 of Kooh Siah is 178 meters. This formation consists of three facies of pure carbonates, basal shale, and evaporative carbonate, which some of them have become dolomitic. There is no hydraulic detachment between the Kagan and Dalan formations and these two formations often form a single reservoir [18].

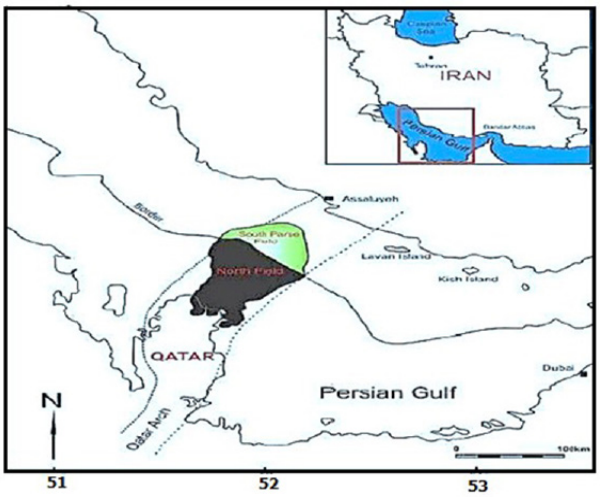

Fig. 1 South Pars gas field and South Pars – Qatar section [4].

The sediments of the Kangan Formation belong to a shallow and energetic marine environment and have high initial porosity [19]. The sample cut of Kangan Formation is subterraneous. Also, Kooh Siah exploration well number 1 is located between the depths 2869 to 3617 meters, and it reaches a thickness of 748 meters. This formation is divided into three sections: lower Dalan, Nar, and the upper Dalan. The lower and upper sections of the formation consist of carbonate sediments, and the middle part is completely anhydrite (Nar part) that separates the lower and upper Dalan.

Materials and Methods

The permeability change in a fractured reservior is controlled by the fracture aperture and its spacing.. Fracture apertures can range in size from very small to very large. When fracture apertures are very small, wall roughness and tortuosity can affect fluid flow. If fracture aperture size is large, two or more fluid phases can flow in the fracture without significantly interfering with each other. The well A which is located in the South Pars gas field andis drilled vertically (the maximum degree of deviation has been reported as 1.5). The drilling mud system used for this well was a water-based mud. This well was started with a 30-inch surface casing, and it was completed with a 7-inch liner in Kangan and Dalan formations. In this study, Geolog 7.1 software with Multimin model was applied to calculate four zones (K1, K2, K3, and K4) of static (such as borehole images and lithological) and dynamic (such as permeability and water saturation) parameters.

In order to interpret the petrophysical charts, information on conventional and advanced petrophysical charts, including Full set, FMI Image log and also information about the core were uploaded on the Geolog software. Several direct and indirect techniques have been proposed, each of which can be used to determine the reservoir characteristics at a fixed point in the reservoir space (in the well site). The general purpose of such an assessment is to obtain a vertical cross-section or profile of each feature. In this study, to interpret the petrophysical graphs, numerical information was compared with reference images. Additionally, homogenization sampling intervals, depth matching, pre-evaluation calculations, environmental corrections, and determination of petrophysical parameters have been done.

These logs show its physical features such as the specific electrical resistance or sonic contrast. The imager provides the possibility for reservoir geologists and oil engineers to identify small-scale phenomena in the wall of the well. Open fractures in formations without clay have conductive appearances in the images. These fractures appear with dark colors because of being attacked by the conductive drilling mud.

In the following, the parameters of the cementation coefficient, water saturation, and uncertainty were determined. Finally, a petrophysical model was developed for four zones (K1, K2, K3, and K4) in Kangan and upper Dalan Formations.

In this study, a multivariate statistical method was used for petrophysical evaluation. The quality of the evaluation results in this method depends on the appropriate selection of the petrophysical parameters. The selection of petrophysical parameters were decided by petrophysical crossover diagrams, core analysis data, well flow experiments, and geological information. Additionally, petrophysical cross-sectional diagrams, sedimentological studies, and core description results were used to determine the lithology and type of minerals in the reservoir formations.

Determination of Lithology by Using Neutron –Density Cross Plot

In the diagram of Figure 2, there are three lines for sandstone (quartz), limestone (calcite), and dolomite. To graphically solve the porosity using this standard diagram, the calculated density values were plotted against neutrons. Three groups of co-porosity lines can be distinguished by drawing, which are obtained by connecting the matrix lines with the same porosity [20]. Based on this cross-lithologic diagram of the Kangan Formation and the upper Dalan, there are generally lime, dolomite, anhydrite, and a small amount of shale, as seen in Figure 2.

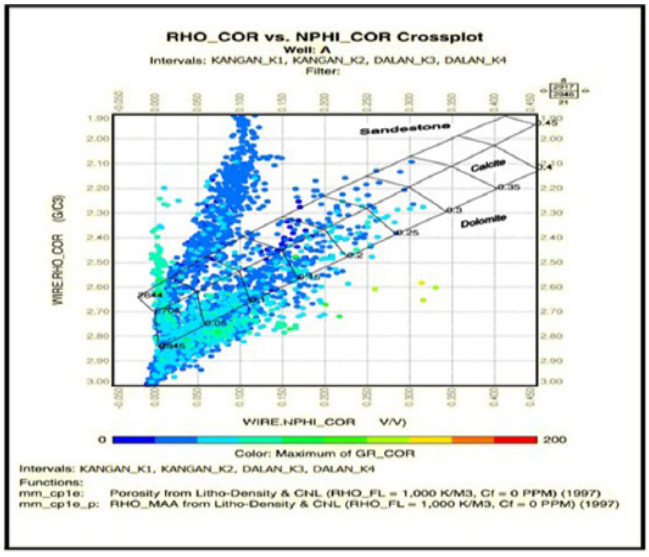

Fig 2. RHO – NPHI crossover diagrams to determine lithology.

Lithology Determination Using MID–Plot, RHO-MAA/ U-MAA Cross Plot

To use this crossover diagram figure 3, first, the logs were corrected for shale and hydrocarbons. Then, the standard (cp-

20) Schlumberger diagram was used to calculate U-maa (Fig 3-a). To determine the lithology with the MID plot, the matrix visionary values (ρma)z and (tma)z were first obtained [21]. For apparent matrix (ρma)z, Schlumberger neutron– density cross plot number (cp-14b) and for (tma) z estimation, Schlumberger neutron–sonic cross plot number (cp-12) were used.

In the Kangan and Dalan Formations, the Apparent values of the matrix (ρma)z, were measured as 2.70 to 2.87 gr per cubic centimeter. Moreover, (tma)z was around 45 to55 micro sec per feet, which shows lime and dolomite stones. Also, the amount of (ρma)z, in some parts Kangan and Dalan Formations, were measured between 2.87 and 3 g per cubic centimeter. In addition, (tma)z in Dalan Formation was plotted in 50-51 micro sec per feet, in which it had the porosity around zero, and it indicates anhydrite. Based on the MID-plot cross-sectional diagram, lithology of Kangan Formation and upper Dalan was composed of limeston, dolomite and anhydrite in well (Fig 3 - b).

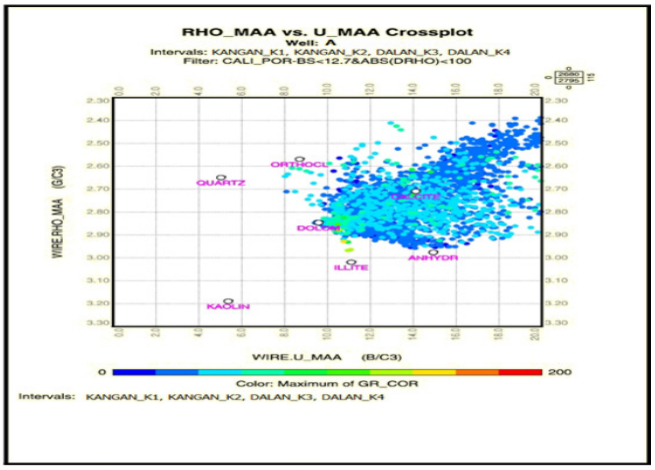

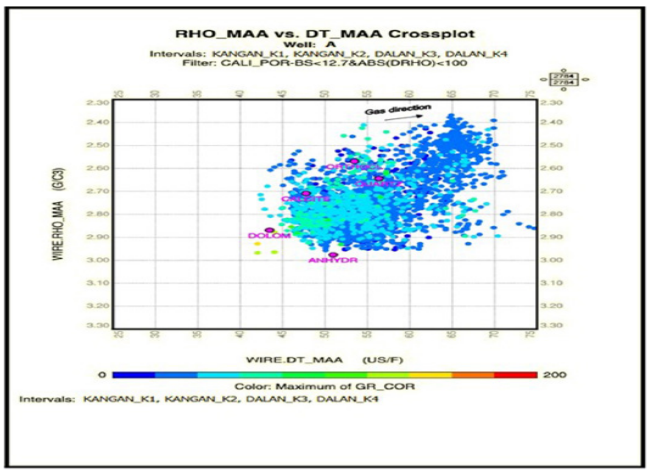

Fig 3. a) RHO-MAA/ U-MAA Cross-sectional diagram for lithological detection b) MID-Plot cross-sectional diagrams view for lithological detection.

Calculation of Water Saturation Degree In Well A

Based on geological data and core studies, Kagan and Dalan Formations have a small volume of shale. The presence of shale minerals in the formation makes it difficult to calculate the water saturation with the Archie model. For this reason, the Indonesian model was used to calculate water saturation in this study. Based on the calculations, the calculated average effective water saturation values for the K1, K2, K3, and the K4 zones were set as 34.5, 48.6, 23, and 76 percentages repectively. Also, the average water saturation calculated in all zones reaches 47%, as seen in Figure 4.

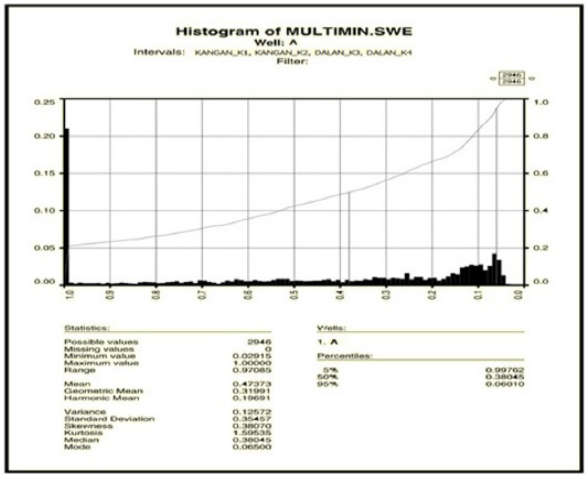

Fig 4 Trends in Effective Water Saturation Changes in K1, K2, K3, K4 zones in Well A.

Shale Volume and Porosity Calculation In Well A

The calculated average shale volume in K1, K2, K3 and K4 zones is respectively 1.19, 0.87, 0.05 and 0.009 percent, which in the K3 and the K4 zones, shale volume is almost zero. Based on the evaluation and analysis of the bar chart of shale volume changes, the studied well has very low shale volume. Additionally, the average volume size of shale of this well in the Kangan Formations and the upper Dalan, was calculated to be 0.39%, as seen in Figure 5-a. Also, in this study, porosity was calculated simultaneously using density, neutron, sonic logs, and core analysis for well A. The average values of total porosity in each K1, K2, K3, K4 zones were calculated as 0.04, 0.087, 0.051, 0.124 percentage, and average effective porosity were 0.04, 0.086, 0.051 and 0.124 percent respectively. As can be seen in this study, total porosity and effective porosity are very similar. The bar chart for the process of effective porosity development is shown in Figure 5, where the average effective porosity of these four zones is 0.08% (Fig 5-b).

Results and Discussion

The Results of FMI Interpretation

FMI log images were processed and interpreted using the Geolog 7.1 software. Also, the steps of loading and image quality control were performed on the intended well. Fullbore micro imager tool, hereinafter referred to as FMI, is taken from the Kangan to the upper Dalan along with other logs. In the process of interpreting the FMI Image log, 26 stylolites, are identified in the studies. These stylolites mainly appear as irregular conductive surfaces on the images. They are observed at almost all logging distances, and they are more frequent in K3 and K4 zones. Stylolites may have originated from parallel layers contact and the overpressure of the upper floors. Moreover, these features are concentrated in a particlura azimuth, but they have a dominant slope in both directions. One of which was detected as northwest, and the other was southwest with 20 degree gradient, as seen in Figure 6.

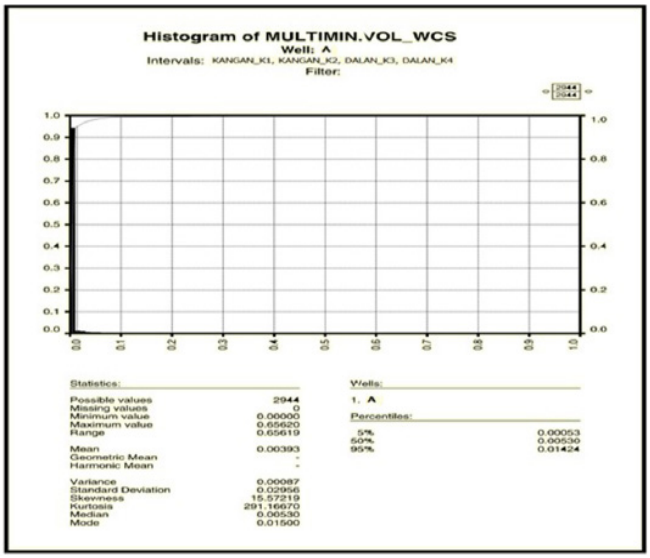

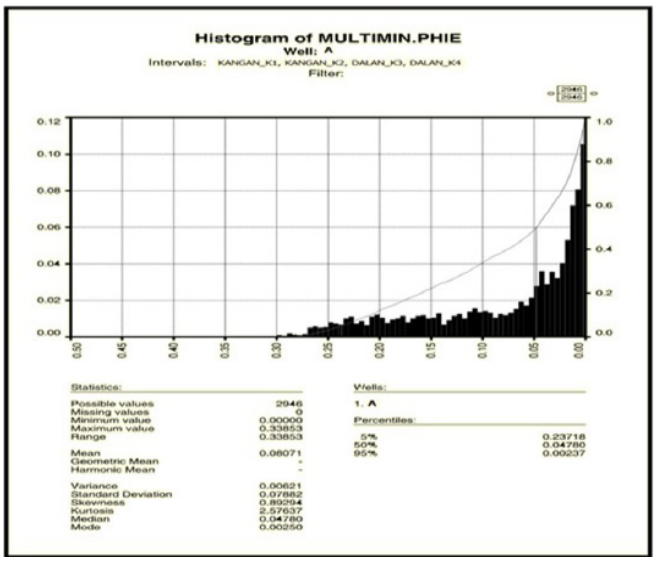

Fig 5. a) Trend of shale volume changes in K1, K2, K3, K4 zones in well A b) bar chart of the process of effective porosity development in K1, K2, K3, K4 zones in well A.

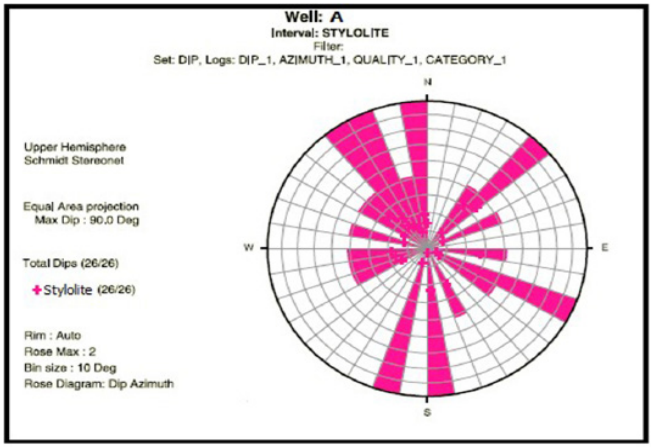

Fig. 6 Stereonet Stylolite in well A with gradient often 20 degrees and northwest-southeast azimuth Azimuth direction.

Conductive fissures in well A, located along the layering boundaries, can be seen on Figure 7 images. These fissures appear to be developed due to temporary changes in the energetic and predominant sedimentary environments of the detrital basins. In general, 35 conductive fissures have been determined during this interval of logging, most of which concentrated in K2 and K4 zones. The most azimuth trend is in the northwest-southeast and northeast-southwest direction with steep gradients (Fig 7-a). Through thestudy of lamination and layering boundary in the well A, it has been found out that 63layers are scattered during the mapping interval. Most lamination and layering have been observed in the K1, k3, and k4 zones. Their gradient is 15 degree, and also their main direction and azimuth trend are northeast (Fig 7-b). Additionally, two cross-beddings could be seen, one of which in the K1 zone with an 8-degree gradient and the azimuth direction of east. Other cross-layering was observed in the K4 zone with a 17-degree gradient and with the azimuth of northeast.

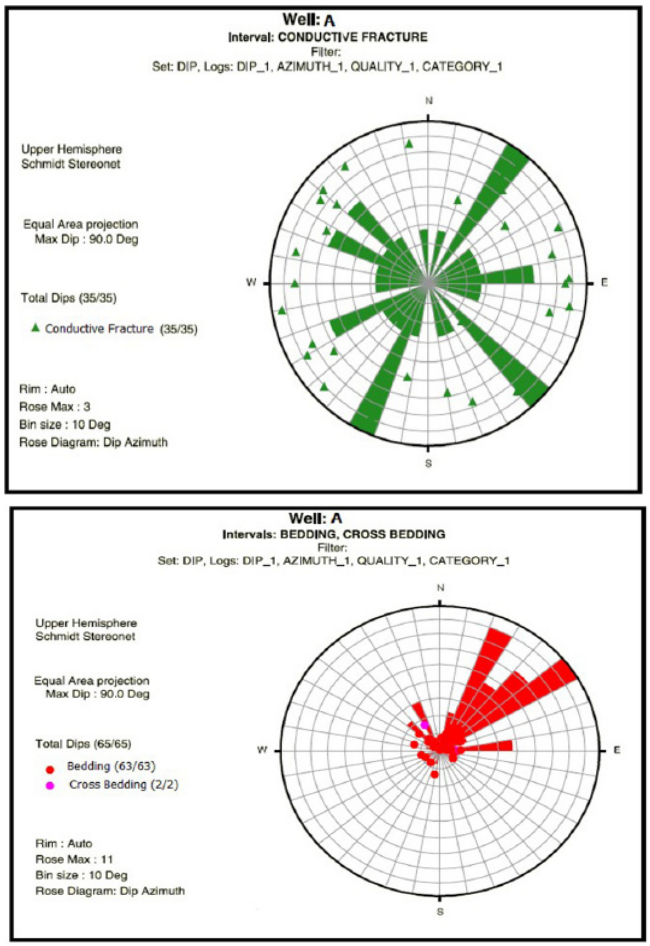

Fig 7. a) Stereonet Conductive Fissures in Well A with 70 Degree gradient and Northeast-Southwest and Northwest - Southeast Azimuth direction. b) Gradient determination of the layers with almost 15-degree gradient and the azimuth of northeast direction in the well A.

In total, there exists 19 open fractures in the logging interval across the four K1, K2, K3, and K4 zones. Most of these fractures are dispersed by 25-40-degree gradients, while four closed fractures are observed in 38, 60, 71and 80-degree gradients in the K1 zone mostlywith northwest-southeast azimuth (Fig 8-a).

Induction fractures caused by the drilling of vertical wellbores are formed parallel with the well axis. However, in wells with low deviation, these fractures have a stepped

shape. Therefore, it is hard to distinguish between the natural fractures and the artificial fractures caused by the drilling. Generally, in vertical wells or wells with low deviations, the orientation of the breakouts is equal to the orientation of the minimum horizontal stress direction. On the other side, the extension of the induction fractures is in the same direction as the maximum horizontal stress.

The most important causes of anisotropy in oil and gas reservoirs are in place tensions, natural fractures and sharp layering boundaries. In this study, anisotropy in the modeling of open and closed fractures are affected on the intensity of porosity distribution and fracture direction.

In the interpretation of this diagram, two breakouts in the K4 zone with a slope of 85 degrees and azimuth direction of southeast were selected. Also, two tensile fractures were observed in the K4 zone with a slope of 85 degrees and azimuth direction of northeast-southwest (Figure 8-b).

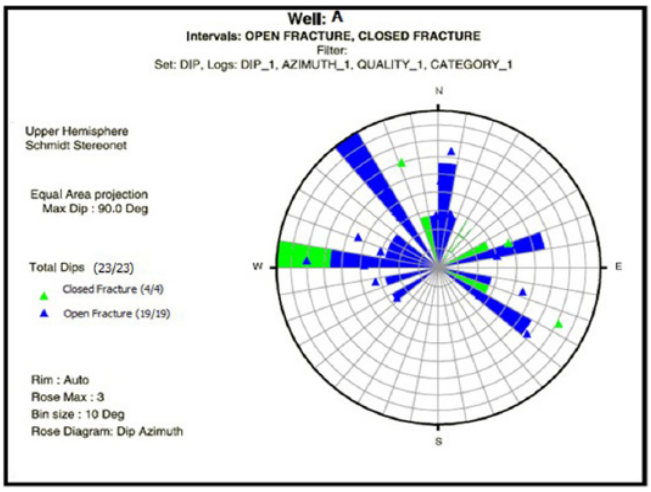

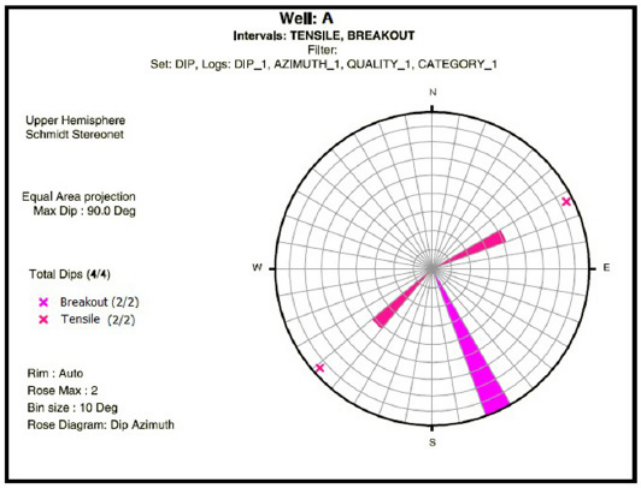

Fig 8. a) Stereonet open and closed fractures in well A with gradients and 25-80-degree gradients and northwest-southeast azimuth direction b) Stereonet Tensile & Breakout in well A with 85-degree gradient and southeast and northeast-southwest azimuth direction.

The Comparing the Results of FMI for Fracture Determination with Core Data

One of the most important sources to study the characterizations of reservoirs are cores especially fracture. Despite the favorable results obtained from the core studies, the costs of preparation and analysis are high. Also, due to some problems associated with coring, such as the low percentage of core recovery at broken and non-compacted areas, and the impossibility of coring in some of the field wells, coring is performed on a limited number of wellbores and fields.

Close fractures in which the spaceof the fractures are filled with dense and non-conducting minerals (calcite and anhydrite), show non-conductive appearances in the images, and it is composed of light brown, yellow and white colors. In this study, the deep distances, in which the drilled cores are investigated, are shown in Fig. 9. The depth of the coring is different from one zone to another. Coring was performed from the depth of 2700 meters to 3300 meters. Also, the amount of core recovery is different, and it is proportional to its fractures.

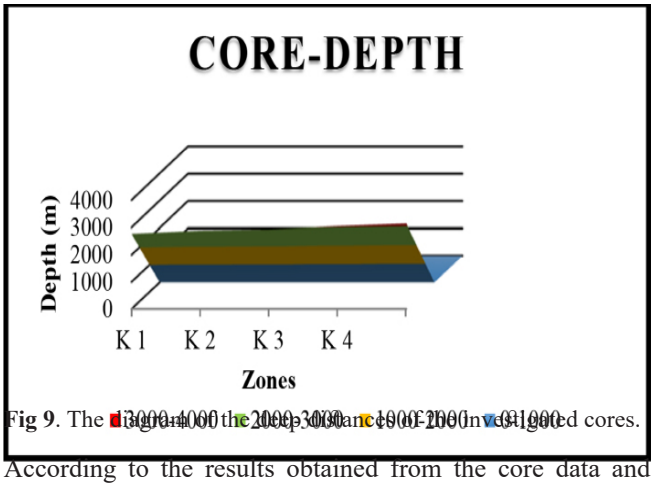

Fig 9. The diagram of the depth distances of investigated cores.

According to the results obtained from the core data and the FMI Image log, the Kangan Formation is an almost fractured carbonate ceservoir. The results shown in Fig.10 indicate that the porosity caused by these fractures ranges from 0.04% to 0.13%. Also, the permeability index in terms of Milli Darcy demonstrated that the zones K4 and K2 have the highest permeability respectively. There is a good relationship between the permeability and porosity in these zones, indicating the presence of micro-fractures and micro-apertures in these two zones. Based on the data on the logs, the fractured zones and the rate of fracture accumulation in these zones were determined.

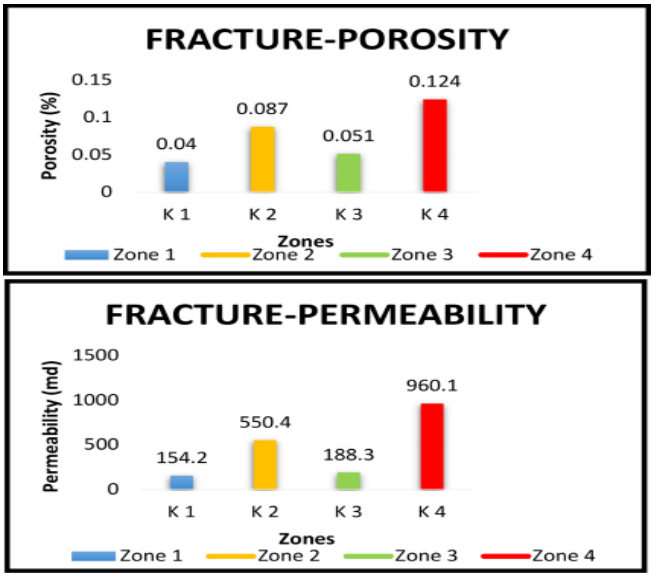

Fig. 10 The column diagram of the average porosity and permeability of the core.

The highest concentration of fractures was in the K2 and K4 zones. These fractures are located in the K2 zone, at depths of 2897-2905, 2910-2915 and 2925-2928 meters. Open fractures and conductive fissures were observed in this zone. K4 zone is severely broken and its fractures are located at a depth of 3050-3140 meters. The fractures in this zone are in the group of open and close fractures, conductive and stylolite fissures, which show more porosity than K2 zone. According to the results obtained by the FMI and experimental analysis on the routine sample of the cores, it was specified that the porosity caused by these fractures is from 0.04% to 0.124%. In zone K4, with high fracture density, the core analysis shows a high porosity, indicating good compliance between the FMI log and the core analysis.

In order to verify this, the images of the cores under study were matched with the images taken from the FMI. As can be seen in Fig.11, the position of the aperture fractures recorded in the log is in good agreement with that of the cores which has been shown in four different states.

For determination of reservoir property including, gradient and azimuth of fractures from petrophysical and FMI image logs were used. Figure 12 show Kangan 1 carbonate horizon, in the deep distance (2776-2885) in well A. Figure 13 shows Kangan 2 and Kangan 3 (upper Dalan horizon) in the (2885-2928) and (2928-3050) deep distances. Figure 14 is a part of the reservoir that is separated from the upper Dalan horizon. The diagram in Figure 14 corresponds to the deep distances of 3050-3140 of the reservoir with the usage of FMI image log, porosity, and water saturation logs. The connection between these figures is that 10 similar items have been examined in all of them and due to different deep distances, their results were obtained differently from each other.

Conclusions

According to the study which has been carried out the following results have been concluded, which they are as follows:

1. The results showed that in K1, K2, K3, K4 zones, at deep intervals where there are stylolite and cross-layering, the highest water saturation and the lowest porosity are observed. Moreover, at deep intervals where there are open and closed fractures, conductive fissures and lamination, low water saturation, and high porosity are observed. The dominant lithology is dolomite and limeston.
2. Based on the FMI Image log, about 200 fractures were identified at the Kangan and Upper Dalan Reservoir intervals, including two tensile fractures, four closed fractures, 19 open fractures, 63 stratifications, two cross-stratification number, 35 conductive fracture number, and 26 stylolite number. Also, 47 unclassified fractures were observed in the two Northwest-Southeast-Northeast-Southwest trends. There are no significant fractures in the Kangan Reservoir zones. Most of the fractures are related to the upper Dalan Reservoir distances.
3. Since fault surfaces, salt domes, and local variations in stratigraphic gradient have never been seen in the FMI image log, fractures may be related to regional tectonic factors.
4. Ultimately, in this study, it was found that the K2 and K4 zones with the highest porosity and least water saturation have higher reservoir quality than the K1 and K3 zones. Also, the K4 zone had the highest fracture density than other zones, which it increased its porosity. Zone K2 with the least thickness (43 meters) had a lower fracture density in comparison with the K4 zone (7 conductive fissures and 2 open fractures). Also, in comparison with other zones, it has low water saturation and high porosity and has a higher reservoir quality than K3 and K1 zones.

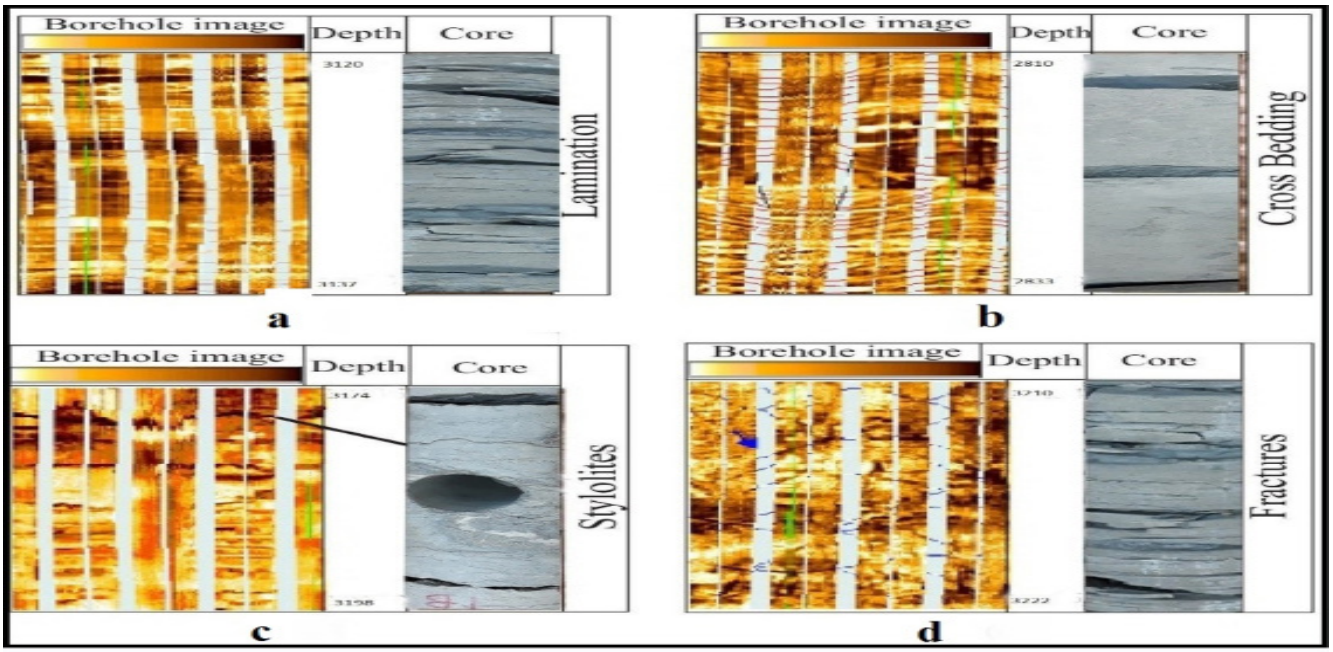

Fig. 11 The image of compliance of the core with the fractures of the FMI log.

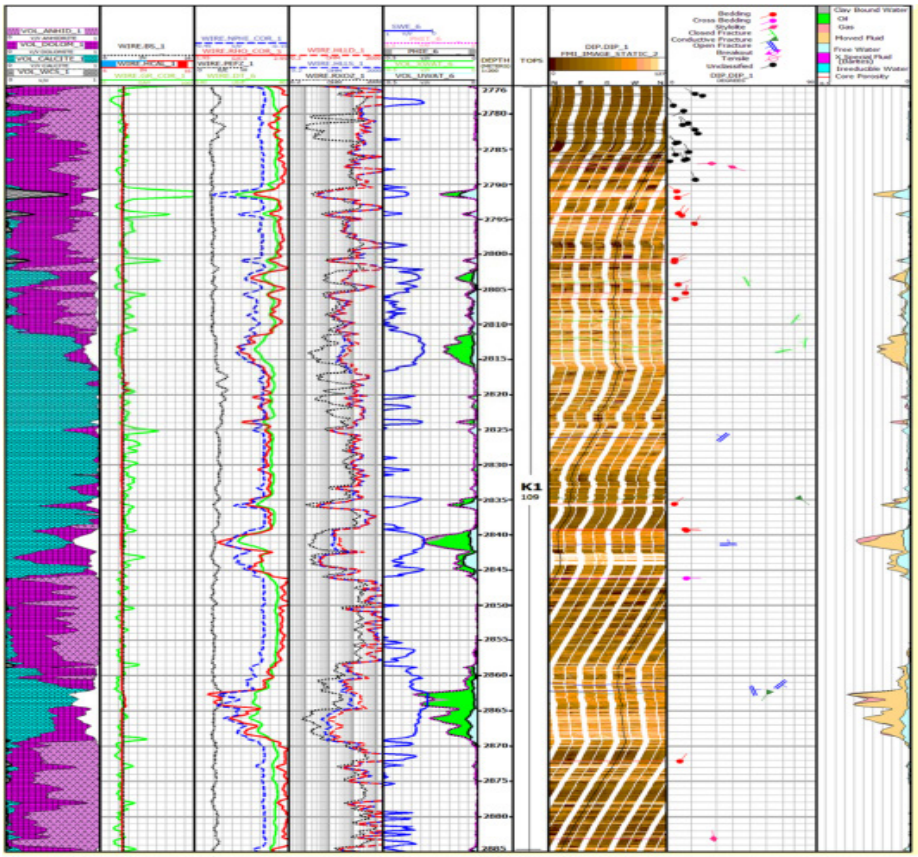

Fig. 12 Determination of reservoir property, gradient and azimuth of fractures using petrophysical and FMI image logs in Kangan 1 carbonate horizon, (2776-2885) deep distance in well A from the left track: Trak 1: Including lithological alterations of the formation Trak 2: Including gamma logs, diameter gauge, bit diameter Trak 3: Including neutron, acoustic, density, photoelectric logs Trak 4: Including resistance logs Trak 5: Including water saturation and porosity Trak 6: Including depth scale in terms of meter Trak 7: Including FMI well imaging Trak 8: Including gauge gradient log Trak 9: Calculating gas porosity and match it with core porosity.

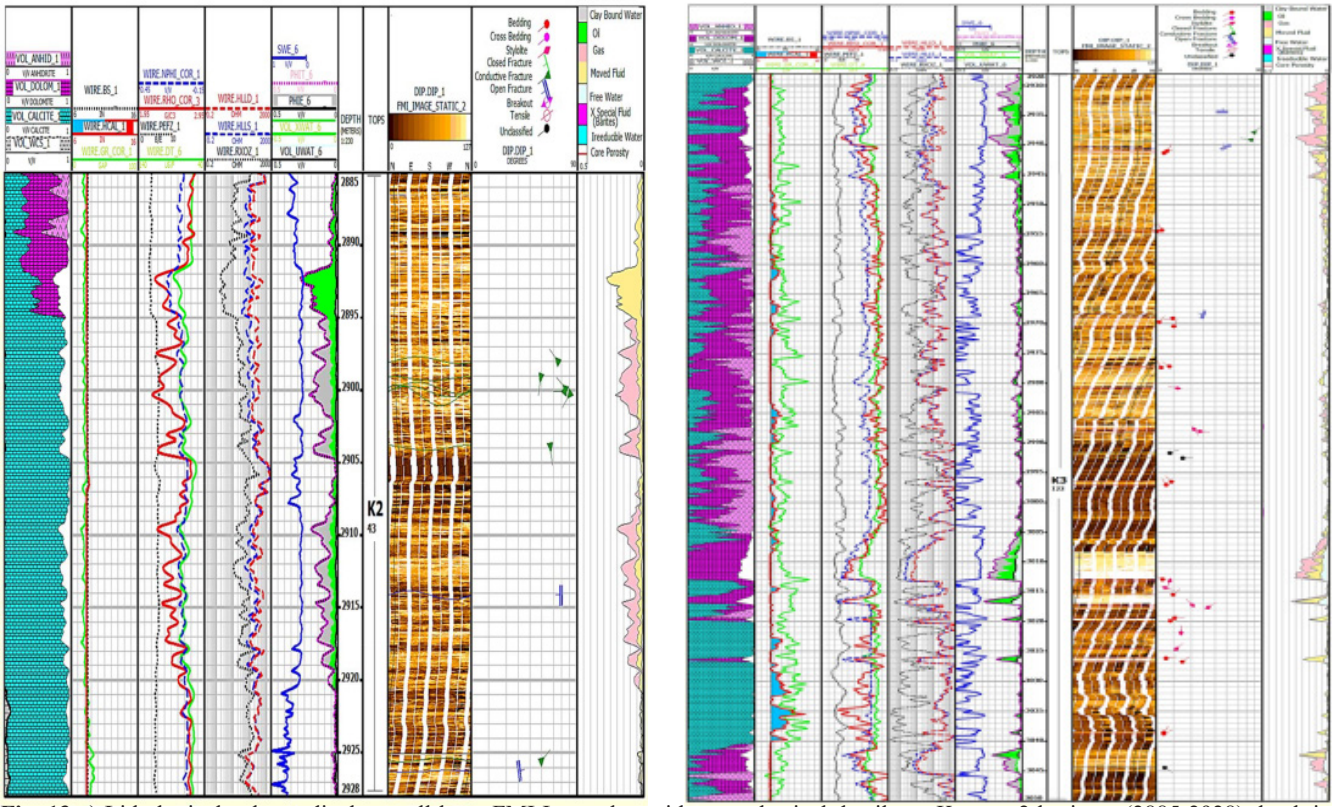

Fig. 13 a) Lithological column display, well logs, FMI Image log with petrophysical details on Kangan 2 horizon, (2885-2928) depth in well A

b) FMI Image log, well logging data and petrophysical evaluation results in Upper Dalan horizon (Kangan 3), (2928-3050) depth in well A.

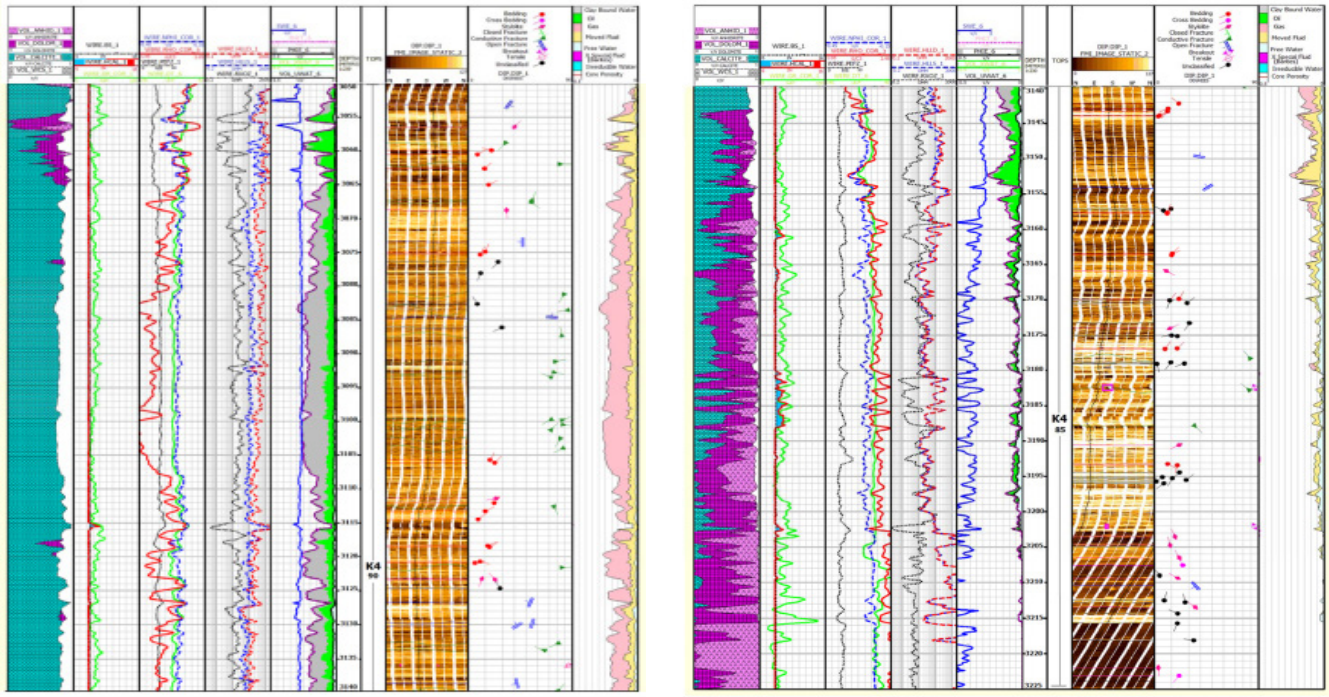

Fig. 14 a) Separation of Reservoir Segment of upper Dalan horizon (Kangan 4), (3050-3140) depth with the usage of FMI Image log, Porosity and water saturation logs in the well A

b) Composite graph with evaluated results such as lithology, production thickness, porosity and hydrocarbon saturation in the upper Dalan horizon (Kangan 4), (3140-3225) depth in well A.

References

1. Mahboobipour H, Bashari A (2006) Petrographic and petrophysical study of permo-triassic carbonate formations (Dalan and Kangan) in Qatar Archipelago in Persian Gulf, 1st ed, Iranian Petroleum Geology, 7-34.
2. Szabo F, Kheradpir A (1978) Permian and triassic stratigraphy, Zagros basin, south-west Iran, Journal of Petroleum Geology, 1: 57-82.
3. Taheri K, Morshedy A (2017) Three-dimensional modeling of mud loss zones using the improved gustafson-kessel fuzzy clustering algorithm (case study: one of the south-western oil fields), Journal of Petroleum Research, 27, 96-5: 82-97.
4. Aali J (2006) Geo chemistry and origin of the worlds largest gas field from Persian Gulf Iran, Journal of petroleum Scienc and engineering, 1-163.
5. Rahimpour-Bonab H, Asadi E, Sonei R (2009) Permian–triassic boundary and its control over reservoir characteristics in South Pars gas field, Persian Gulf: Geological Journal, 44: 341–364.
6. Soleimani M, Jodeiri Shokri B, Rafiei M (2017) Integrated petrophysical modeling for a strongly heterogeneous and fractured reservoir: Sarvak Formation, SW Iran, Natural Resources Research, 26: 75–88.
7. Tokhmechi B, Memarian H, Rezaee R (2010) Estimation of the fracture density in fractured zones using petrophysical logs, Journal of Petroleum Science and Engineering, 72, 1–2: 206-213.
8. Soleimani M (2017) Naturally fractured hydrocarbon reservoir simulation by elastic fracture modeling, Petroleum Science, 14:, 286–301.
9. Ja'fari A, Kadkhodaie-Ilkhchi A, Sharghi Y, Ghanavati K (2011) Fracture density estimation from petrophysical log data using the adaptive neuro-fuzzy inference system, Journal of Geophysics and Engineering, 9: 105–114.
10. Abdideh M, B Birgani N, Amanipoor H (2013) Estimating the reservoir permeability and fracture density using petrophysical logs in Marun Oil Field (SW Iran), Petroleum Science and Technology, 31, 10: 1048-1056.
11. Soleimani M (2017) Well performance optimization for gas lift operation in a heterogeneous reservoir by fine zonation and different well type integration", Journal of Natural Gas Science and Engineering, 40: 277-287.
12. Shahinpour A (2013) Borehole Image log analysis for sedimentary environment and clay volume interpretation, Norwegian University of Science and Technology, Department of Petroleum Engineering and Applied Geophysics, 84: 1-53.
13. Rahimpour-Bonab H, Enayati-bidgoli A.H, Navidtalab A, Mehrabi H (2014) Appraisal of intra reservoir barriers in the Permo-Triassic successions of the Central Persian Gulf", Offshore Iran: Geological Acta, 12: 87-107.
14. Rezavand N, Jahani D, Asilian H (2016) Facies, sedimentary environment and sequence stratigraphy of dalan formation in South Fars, Iran (Qatar-South Fars Arch) Well ASL-A, Open Journal of Geology, 6: 944-962.
15. Taheri, K., Rasaei, M. R., and Ashjaei, A. (2018). Study the role of drilling mud loss modeling and FMI log in determining Asmari reservoir fractures in one of the oil fields in Southwest Iran. Iranian Journal of Petroleum Geology, 14(7),18, doi:rimag.ricest.ac.ir/fa/Article/33847.
16. Lai J, Wang G, Fan Z, Chen J, Qin Z, Xiao C, Wang S, Fan X (2017) Three-dimensional quantitative

fracture analysis of tight gas sandstones using industrial computed tomography, Scientific Reports, 7, 1: 1825.
17. Aghli G, Soleimani B, Tabatabai SS, Zahmatkesh I (2017) Calculation of fracture parameters and their effect on porosity and permeability using Image logs and petrophysical data in carbonate Asmari reservoir, SW Iran, Arab Journal Geoscience, 10: 265.
18. Motiei H (1995) Zagros oil geology, 1 and 2, Book Compilation Plan, Geological Survey of Iran, 1010.
19. Motiei H (1993) Geology of Iran, Zagros stratigraphy, Geological Survey and Mineral Exploration of Iran, 583.
20. Rezai M. R, Chehraazi A (2006) Principles of enhanced oil recovery and interpretation of well logistics, Tehran University Press, 699.
21. Clavier C, Rust DH (1976) MID Plot: A new lithology technique, Log Analyst, 17, 6: 16.